Ceramics International 24 (1998) 333–339
© 1998 Elsevier Science Limited and Techna S.r.l.
Printed in Great Britain. All rights reserved
PII: S0272-8842(97)00019-9
0272-8842/98 $19.00 + .00

Crystal Orbital Scheme for Si_3N_4

Lubomír Benco*

Institute of Inorganic Chemistry, Slovak Academy of Sciences, Dúbravská cesta 9, SK-842 36 Bratislava, Slovak Republic

(Received 1 July 1996; accepted 20 November 1996)

Abstract: The crystal orbital (CO) scheme is constructed for β-Si_3N_4 to display the bonding in the solid compound. The electronic band structure is obtained within the extended Hückel tight-binding approach for periodical systems. For the purpose of comparison features of the electronic structure are contrasted for a series of SiC, Si_3N_4, and SiO_2. Partial DOS are displayed to highlight orbital interactions. Combined with bonding properties of states they are used to assign simplified interaction diagram consisting of atomic energy levels, total DOS distribution and interaction lines. The interaction scheme provides well-arranged synoptical picture showing fundamental factors responsible for the final distribution of energy states. Via the CO scheme the bonding in β-Si_3N_4 is displayed in the form understandable to people with no knowledge of quantum mechanics. © 1998 Elsevier Science Limited and Techna S.r.l. All rights reserved

INTRODUCTION

The electronic structure of crystalline Si_3N_4 has been documented by several groups of researchers using empirical or semiempirical approaches,[1–5] first-principles not self-consistent[6] and also self-consistent method.[7–9] Calculations are thoroughly reviewed by Robertson.[10] Band structures and the density of states (DOS) are presented for β-Si_3N_4 (Refs 1–5). Electronic structures of both α- and β-phase are compared in Refs 6 and 9. Ching *et al.* illustrate that calculated spectrum of energy states compares well with XPS experiments.[11,12] The total and partial DOS of α-Si_3N_4 are only slightly different from that of β-Si_3N_4. The low resolution of the XPS-type experiments and surface admixtured amorphous phase prevents the detailed comparison of two structures. Four bands of occupied states, clearly visible irrespective of α-, β-, or amorphous phase, apparently originate from interactions between nearest neighbours within basic structural unit of SiN_4 tetrahedra.

The four main peaks have been described in terms of the band structure, DOS, partial DOS and charge density maps. These classical tools of the solid state physics and chemistry provide valuable, but only partial characteristics of a solid as seen from various points of view. Silicon nitride has been important industrial material. Since all material properties depend ultimately on the electronic structures, detailed information on the energy-band structure can advance basic understanding about the solid compound. Most of people treating this material in many diversified applications are non-professionals to the field of theoretical methods. Results originated from the solid state theory therefore should provide simple explanation of the bonding and indicate the relation of the electronic structure and properties of solid materials. A lot of work in learning how to think and understand chemical bonding in solids on the basis of interatomic interactions has been initiated in Hoffmann's group.[13,14] They use to seek out of simple orbital explanations and relationships between the structure at hand and all other possibly related systems. Following their strategy the crystal orbital (CO) scheme was introduced recently[15,16] in which the analysis of orbital interactions results in one simple figure. The figure integrates essential features of the electronic structure stressing the role of the chemical bonding. Based on the DOS distribution the scheme represents simplified interaction diagram

---

*Present address: Institut de Chimie Inorganique, Universite de Fribourg, Perolles, 1700 Fribourg, Switzerland.

providing the explanation why the spectrum of states is shaped the way it is.

In this work the crystal orbital scheme for Si_3N_4 is constructed based on the electronic structure of the β-phase. Details on the structure and the computational method are followed by results (DOS and partial DOS) briefly summarized to the extent necessary to show orbital interactions. Finally, an analysis of bonding properties of states is shown to provide the ground for the understanding of the bonding and setting up the crystal orbital scheme for Si_3N_4.

STRUCTURE AND COMPUTATIONAL DETAILS

The crystal structure of β-Si_3N_4 is described by Hardie and Jack[17] (a phenacite-type structure, space group symmetry $P6_3$). Each Si atom is in the center of irregular tetrahedron of N atoms. The tetrahedra share corners in such a way that each N atom is common to three tetrahedra (Fig. 1(a)).

Three-dimensional CO calculations[18] are performed within the extended Hückel approach[19,20] (parameters from Refs 21 and 22, single crystal structural data from Ref. 23). The asymmetric unit of the Patterson space group $P6/m$ is employed as an integration domain in the **k** space[24] (Fig. 1(b)). A 52 **k** point mesh is used to compute the density of state curves and crystal orbital overlap populations.

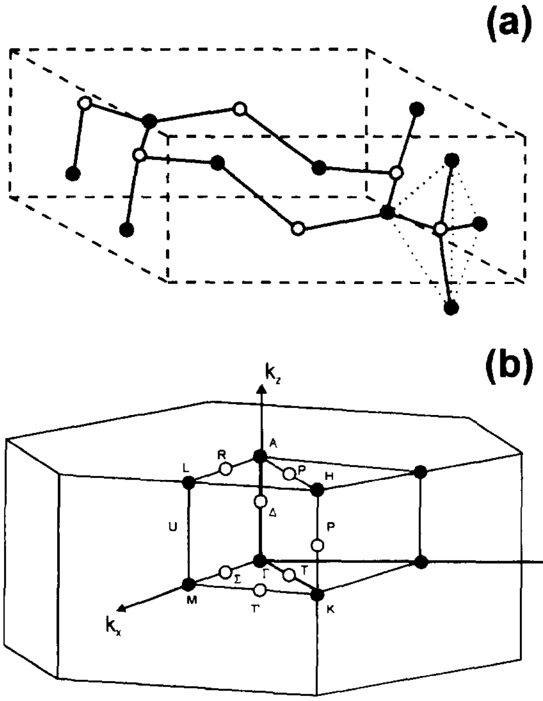

Fig. 1. (a) The atomic arrangement of the unit cell of β-Si_3N_4. The full (open) circles represent nitrogen (silicon) atoms. Two N atoms from neighbouring cells are included to highlight the tetrahedral coordination sphere of silicon (dotted lines). (b) The Brillouine zone for the hexagonal structure and the asymmetric unit of the Patterson space group $P6/m$. High symmetry elements of the ireducible wedge are indicated by full (points) and open (axes) circles.

RESULTS AND DISCUSSION

Total density of states

Calculated total DOS curve for β-Si_3N_4 is shown in Fig. 2. For the purpose of comparison this curve is displayed for a series of structures made of SiX_4 tetrahedra (X = C, N, and O). The methodology used to describe the electronic structures is approximate,[19,20] not reliable quantitatively. An energy gap separating the valence band (VB) top states and the minimum of the conduction band (CB) is always exaggerated. Nevertheless, the methodology provides a conceptual basis for understanding of electronic structures.[13,14]

Three bands separated by sizable gaps dominate the valence region of all three compounds (Fig. 2). The lower VB and the upper VB (from the left) are followed by the CB. First two of them are bands of occupied states. According to dominant components they are usually referred to as *s* and *p* bands (for more detailed explanation see the following paragraph). Dashed and dotted lines in Fig. 2 indicate states due to equivalent orbital interactions (see orbital interactions below). The Fermi level (E_F)—the highest occupied energy level—falls at the edge of the VB. Note that states in Si_3N_4 (from the left up to the Fermi level) show typical four peak structure in accordance with XPS experiments[11,12] and total DOS presented by

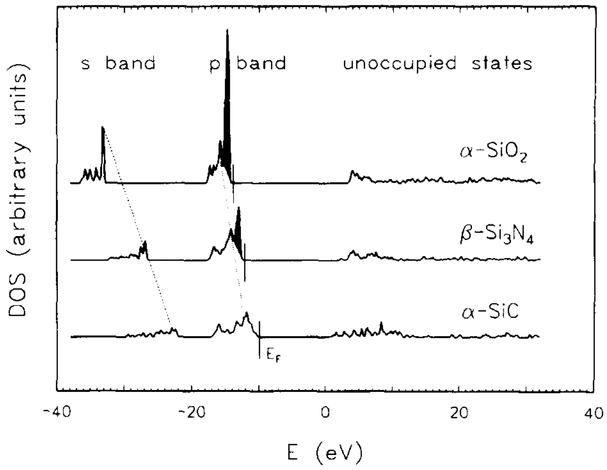

Fig. 2. The comparison of the total DOS for α-SiC, β-Si_3N_4, and α-SiO_2 (normalised to one formula unit); Vertical lines located at the edge of the valence band indicate the position of the Fermi level of the corresponding compound (E_F). the filled area highlights states originated from nonbonding electrons.

other groups.[1–9] Because VBs are completely filled, α-SiC, β-Si_3N_4, and α-SiO_2 are stable systems. On going from SiC to SiO_2 the total DOS exhibits enlarged separation of highest occupied and lowest unoccupied states. This increasing of the energy gap indicates enhanced thermal stability. As apparent in Fig. 2, the large energy gap is due to the band position but depends also on the width of bands (band positions are discussed in the last section of this paper). Relatively narrow bands in SiO_2 also stand for factors contributing to the high thermal stability of this compound. For α-SiC, β-Si_3N_4, and α-SiO_2 the widths of occupied bands are summarised in Table 1. Other property of a material closely related to the width of bands is hardness. The hardness critically depends on the strength of bonds. The bondstrength is driven by the covalency of the bonding and the degree of covalency itself is reflected in the electronic structure of compounds. The more covalent bonding, the larger bandwidths of corresponding bands in bandstructures.[13,14,25,26] As the hardness of compounds has been assessed according to the corresponding bulk modulus,[27,28] (the bulk modulus of an ideal solid is defined as the resistance of a material towards elastic deformations) there exists close relation between width of bands in electronic structures and bulk moduli. Last column in Table 1 demonstrates this relation. Both *s* and *p* bands are considerably broadened from SiO_2 towards SiC. The trend in increasing the bandwidth corresponds well with increasing bulk moduli.

In SiC the pronounced band broadening results in considerably reduced energy gap (compared to SiO_2 and Si_3N_4) and this material appears a wide bandgap semiconductor.[29] As the crystalline long-range order plays no role in determining the overall electronic structure, semiconducting properties are intrinsic to all SiC polytypes.

Partial DOS and orbital interactions

The DOS curves in Fig. 2 show multiple structures in all three band regions. Such fine structures delineate details of the bonding interactions. The gross features of the calculated DOS spectra, which are similar for all three compounds, are in good agreement with the experimental UPS and XPS measurements.[11,12,30–32] Fine structures especially for deeper lying levels are in experimental spectra not present because of technical limitations and/or due to a complex background in the photoionization process. Numerous band structure calculations reported so far, however, display DOS structures, which can be assigned to orbital-to-orbital interactions. The investigation of orbital interactions needs the band decomposition of orbital-projected components. Such decompositions (appearing, for example, in Refs 6 and 9) is detailed in Fig. 3 for β-Si_3N_4. In covalent bonding the states (both bonding and antibonding) contain components of both interacting partners. In decomposition of states into orbital contributions covalent interactions are thus easily recognized according to the mirroring of interacting components on the energy scale. As SiC, Si_3N_4 and SiO_2 are highly covalent systems this mirroring allows the classification of states according to orbital interactions. Figure 4 shows orbital interactions between the central silicon atom and the nonmetal atom in the corner of the tetrahedron.

Table 1. Width of occupied bands and bulk moduli of α-SiC, β-Si_3N_4, and α-SiO_2

	Bandwidth (eV)		
	s band	*p* band	B_0 (GPa)*
α-SiC	7.5	6.8	430
β-Si_3N_4	5.7	4.9	120–330
α-SiO_2	3.5	3.3	74

*Bulk moduli B_0 according to Ref. 40, pp. 808, 815, and 330 for SiC, Si_3N_4, and SiO_2, respectively. A value for sintered α-SiC is reported. Broad range of values for Si_3N_4 covers different material types.

Though the following analysis of orbital interactions is demonstrated for Si_3N_4, conclusions are valid also for SiC and SiO_2, because interactions within similar building units (SiX_4 tetrahedra) give rise to similar dispersion of states (Fig. 2 and Refs 1–12 for Si_3N_4, Refs 33 and 34 for SiC, Refs 35 and 36 for SiO_2). The partial DOS (Fig. 3) show that states of the *s* band which are dominated by the

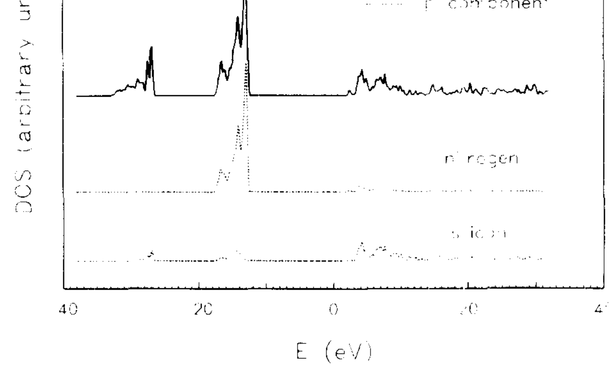

Fig. 3. The decomposition of states of Si_3N_4 into orbital components. The mirroring of states on the energy scale (silicon vs nitrogen) indicates a covalent interaction. Note that each structure of DOS is due to the orbital interaction except the hight narrow sub-band at the edge of the *p* band. These states of nonbonding electrons originated from the nitrogen *p* orbitals have no counterpart on silicon.

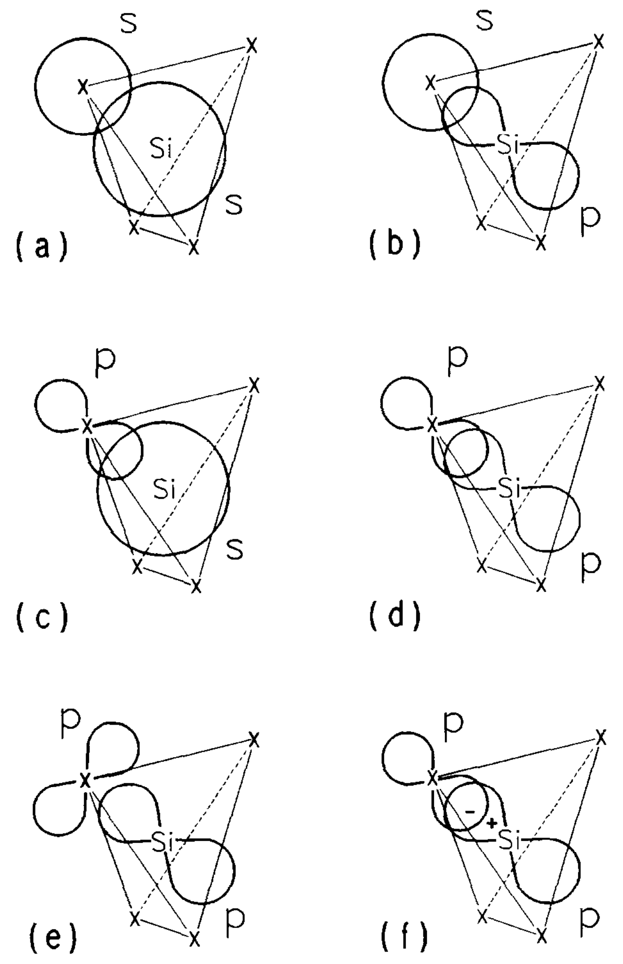

Fig. 4. Orbital interactions inside the SiX_4 tetrahedra displayed for the central silicon atom and one atom situated in the corner. (a–d) Bonding interactions. (e) The nonbonding interaction. Non-overlapping nonmetal orbitals accommodate nonbonding electrons. (f) The overlap of charge densities with opposite signs gives antibonding states.

N(2*s*) component are clearly due to two kinds of interactions. The N(2*s*)-to-Si(3*s*) interaction (Fig. 4(a)) gives rise to low intensity states spread over several eVs at the low energy side of the band. These represent the deepest lying energy states of the valence region. The states concentrated in relatively narrow sub-band at the high energy side of the *s* band (in Fig. 2 indicated by dashed line) are due to the N(2*s*)-to-Si(3*p*) interaction (Fig. 4(b)). Different bandwidths of these two sub-bands are caused by different atomic orbital overlaps (a tetrahedral arrangement allows only limited overlap of central Si *p* orbitals with *s* orbitals of coordinated N atoms).

The distribution of states inside the *p* band displays similar pattern. The structure shows two distinct sub-bands (SiC) supplemented with another pronounced subband (filled area in the spectra of Si_3N_4 and SiO_2 in Fig. 2). This band contains only *p* states of the more electronegative atom (nitrogen) admixtured with two components coming from silicon. States of the subband at the low energy side are due to the N(2*p*)-to-Si(3*s*) interaction (Fig. 4(c)). States of the next subband originate from N(2*p*)-to-Si(3*p*) interaction (Fig. 4(d)). Note that only states indicated by a dotted line (Fig. 2) show mirroring of N(2*p*) vs Si(3*p*) states in Fig. 3. Having no bonding counterparts, the highest occupied states, highlighted by the filled area in Fig. 2, appear to be nonbonding ones. As demonstrated in Fig. 4(e), these nitrogen *p* orbitals do not overlap with orbitals of the neighbouring silicon atom.

The unoccupied states are spread over large energy interval and do not show characteristic features. Nevertheless, the lowest unoccupied states contain orbital components indicating antibonding interaction of Si(3*p*) and N(2*p*) orbitals. These states are due to the negative overlap of orbitals (note opposite signs of atomic wave functions in Fig. 4(f)).

Bonding properties of states

Solid state allows more interatomic interactions compared to molecules because of closer packing in three dimensions. Atoms in solids thus often simultaneously participate in several kinds of interaction, some of them can be competitive (e.g. the *pd* vs *dd* competition in transition metal carbides and nitrides[37,38].) Density of states represents the sum of all interactions. Investigating bonding properties of states one must therefore consider all relevant interactions. Any state (defined by its position at energy scale) inside a band consists of contributions which in principle can show bonding, antibonding, and nonbonding properties depending on interacting counterparts. The global terms like, for example, "bonding states at −11 eV" indicating bonding properties without predefined interacting bodies are inadequate and might lead to an erroneous interpretation (an example of erroneous conclusions about the bonding in transition metal carbides and nitrides[39] is given in Ref. 15).

An obvious procedure in investigation of bonding properties of states is the calculation of Mulliken overlap population for all states in a certain energy interval.[13,20,25] It is positive (negative) for bonding (antibonding) states and approaches zero for nonbonding ones. Figure 5 shows COOP (crystal orbital overlap population) curves for α-SiC, β-Si_3N_4 and α-SiO_2 within the energy interval covering the *p* band. The total DOS is displayed for reference to indicate where the bands of states are located (the scale for the DOS differs from that for COOP curves). The COOP quantity is overlap population-weighted DOS displaying bonding properties in graphical form.[13,20,25]

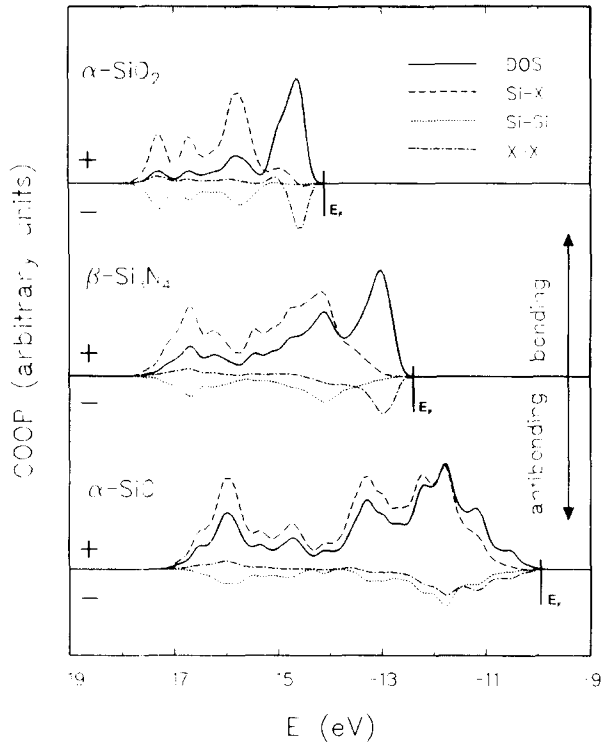

Fig. 5. The COOP curves for the *p* band of α-SiC, β-Si_3N_4, and α-SiO_2. The dashed line indicate properties of states due to the interaction of nearest neighbours. Note that they are all bonding (positive values). the interaction of next-nearest-neighbours is slightly anti-bonding for the Si—Si interaction (dotted line). The X-X interaction (X = C,N,O; dot-dashed line) is slightly bonding. Topmost occupied states show the antibonding behaviour due the repulsion of lone electron pairs in Si_3N_4, and SiO_2. The total DOS (full line) is displayed for reference.

Dashed lines display the COOP for the interaction of nearest neighbours (Si-to-X). They indicate that in all three systems most bonding states come from the interaction of nearest neighbours. In Si_3N_4 and SiO_2 this curve is positive throughout the whole *p* band, but falls to the zero line within the sub-band situated at the higher energy side (just below E_F). This demonstrates the nonbonding character of these highest occupied states. Such nonbonding states participate only in electrostatic interactions. Increased number of nonbonding states (filled area Fig. 2) causes increased ionicity of the bonding and drives properties of materials (cf. bulk moduli in Table 1). Intriguing feature is that none Si-to-X antibonding states (X = C, N, O) appear within the *p* band in these compounds. All Si-to-X bonding states are occupied already in SiC (eight electrons per four bonds). Additional electrons in Si_3N_4 and SiO_2 turn nonbonding but not antibonding. The tendency of electrons to avoid filling of antibonding states gives rise to modified arrangement of the SiX_4 tetrahedra in the structure. To keep *p* electrons nonbonding an overlap of orbitals must diminish. This is achieved by increasing the Si–X–Si angle from ≈ 110° in α-SiC to ≈ 120° in β-Si_3N_4 and to ≈ 144° in α-SiO_2. The structures lower their symmetries (from $P6_{3mc}$ to $P6_3$ and to $P3_21$) and become more open to accommodate increased number of non-overlapping lone electron pairs. This capacity of structures to prevent electrons from filling of antibonding states represents another important circumstance closely relating the high thermodynamical stability of these compounds.

The curves for second neighbours (silicon–silicon and nonmetal–nonmetal) are much closer to the zero line (Fig. 5). This demonstrates diminished role of the bonding between second neighbours compared to nearest neighbours. The Si-to-Si curves (dotted) show weak antibonding interaction within both bonding sub-bands (Fig. 5, sub-bands of Si_3N_4 at ≈ −17 eV and ≈ −14 eV and corresponding sub-bands in SiC and SiO_2). The dash-dotted curves indicate that all states of the *p* band are slightly nonmetal-to-nonmetal bonding except the topmost occupied states (Fig. 5, right sub-band just below E_F in each compound). These show antibonding nonmetal-to-nonmetal interaction. In SiC the states located at ≈ −12 eV display a weak carbon-to-carbon interaction. In Si_3N_4 states at ≈ −13 eV, occupied by lone electron pairs, are much more nitrogen-to-nitrogen antibonding (compared to SiC). In SiO_2 a considerable amount of the electron density is Si–O nonbonding. The dash–dotted curve shows that nonbonding states are strongly antibonding in oxygen-to-oxygen interactions.

Crystal orbital scheme

The crystal orbital scheme is simplified interaction diagram comprehending all particular solutions reported in previous paragraphs (Figs 2–5). In Fig. 6 the CO scheme is shown for Si_3N_4. It consists of three components: (i) the total DOS displayed on the real energy scale; (ii) atomic energy levels; and (iii) interaction lines connecting energy states before (atomic) and after (solid state energy states) the bonding. Horizontal lines within the DOS denote band and/or sub-band maxima (centres of mass for broad bands).

The scheme shows which levels take part in the bonding (*s* and *p* levels of both silicon and nitrogen atom). Interaction lines indicate orbital interactions giving rise to the splitting of atomic orbitals into a multiplet of levels. Bonding properties of states are characterised by the direction of interaction lines. Lines going downwards indicate stabilization (compared to the atomic position) and bonding character of states. Levels shifted upwards are antibonding. Nonbonding states reside at their

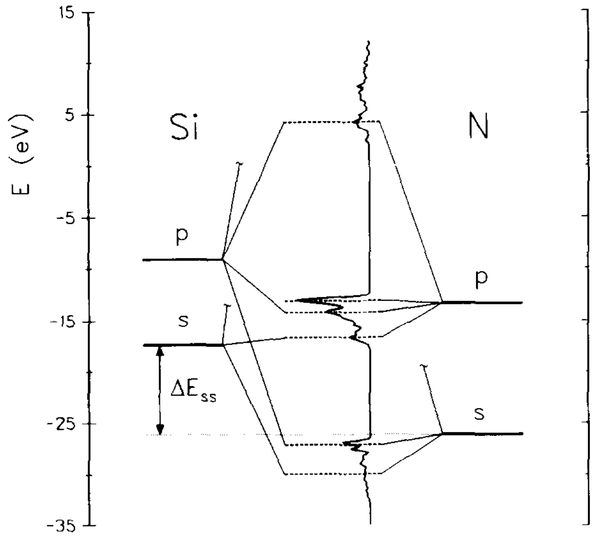

Fig. 6. The crystal orbital scheme for Si_3N_4. The scheme consists of the total DOS, atomic energy levels and interaction lines. Interaction lines show the origin of states and indicate their bonding properties. States shifted downwards (relative to the atomic position) are bonding. Note that highest occupied states are clearly nonbonding as they reside at their atomic position. States shifted upwards are antibonding (destabilised). Truncated interaction lines indicate off scale position of antibonding states. ΔE_{ss} shows the energy separation for the Si(3*s*)-to-N(2*s*) orbital interaction.

atomic position (note the band of highest occupied states originated from nitrogen lone electron pairs in Fig. 6).

Several features within the CO scheme demonstrate simultaneously the degree of the covalency/ionicity of states. Only states having both bonding and antibonding counterparts are covalent. In the valence region of Si_3N_4 all states except the band of nonbonding states (see above) are covalent. The nonbonding states reside exclusively at the more electronegative nitrogen atom having no counterparts for covalent bonding. Therefore they take part in the bonding only via electrostatic (ionic) interactions. The stabilizing shift of occupied states (compared to atomic positions) scales with the degree of covalency. Note that different states show different covalency. The degree of covalency reflects also in bandwidth—more covalent bonding causes spreading of states over broader energy intervals. Extremely narrow band of nonbonding states, contrary, demonstrates their ionic character.

The scheme underlines the role of ΔE—the energy difference between interacting atomic levels (in Fig. 6 ΔE_{ss} indicates the energy difference between *s* levels of the two neighbouring atoms). ΔE is proved one of the governing factors of the bonding. The smaller value of the ΔE gives rise to the higher covalency (in a supercovalent system like diamond and solid silicon $\Delta E = 0$). Within the *p* band states due to both *pp* and *sp* interactions (sub-bands at ≈ -13 and ≈ -17 eV) show similar energy matching—$\Delta E_{pp} \cong \Delta E_{sp} \cong 4$ eV. Therefore their degree of covalency is similar. The *s* band, contrary, consists of states of two kinds. Less stabilised upper states concentrated within the narrow energy iterval at ≈ -27 eV are rather ionic ($\Delta E_{ps} \cong$ 17 eV). More stabilised states, spread over the broad energy interval down to ≈ -33 eV, are apparently more covalent ($\Delta E_{ss} \cong 9$ eV).

The values of ΔE, determined by positions of atomic levels, closely relate to electronegativity values of interacting elements. The larger ΔE corresponds to the larger difference in electronegativities. Note that atomic levels of the more electronegative atom (nitrogen) drive the location of occupied states of the solid compound on the energy scale. Both the *s* and the *p* band of Si_3N_4 are located close to the nitrogen atomic positions, slightly stabilised as already described above. In general the larger is the value of ΔE, the smaller is the contribution from orbitals of the less electronegative atom. Occupied states are therefore dominated by the component coming from the more electronegative atom. In Si_3N_4 rather large values of the energy difference ($\Delta E \cong 9$ eV, and $\cong$ 4 eV for the *ss* and the *pp* interaction, respectively) indicate that states of the nitrogen atom must dominate the bonding. Partial density of states (Fig. 3) demonstrate that the band composition corresponds well with the value of the ΔE. In spite of the fact that the CO scheme does not show partial DOS (to keep it as simple as possible) the band composition is apparent from values of the ΔE.

CONCLUSIONS

Electronic structures are reported for a series of solid compounds SiC, Si_3N_4, and SiO_2. A simple comparison of total DOS demonstrate the increased thermal stability of SiO_2 on one side and the higher hardness of SiC on the other side. Particular solutions of electronic structures are integrated into one simple figure called the crystal orbital scheme. The step by step construction of the scheme is demonstrated for Si_3N_4 to be easily reproduced for other solids. The CO scheme shows characteristic features like bands, sub-bands, energy gaps, bandwidths, etc. Instructively and in a well understandable way are displayed orbital interactions responsible for stabilising (destabilising) shifts of energy levels and splitting of levels into components with various bonding properties, providing also the comparison of iono/covalent properties of states. Comprehending many particular solutions the CO scheme represents the complete picture of the chemical bonding in the solid compound.

ACKNOWLEDGEMENTS

M. Liška is acknowledged for encouragement. Thanks are due to I. Proks and P. Šajgalík for helpful discussions, and to Z. Pánek and Z. Lenčeš for their help with thermodynamical data. Acknowledged is partial financial support from the US—Slovak scientific and technological program No. 94039, Slovak Grant Agency VEGA (grant No. 1172), and from the Human Capital and Mobility programme of the European Community.

REFERENCES

1. MARTIN-MORENO, L., MARTINEZ, E., VERGES, J. A. & YNDURAIN, F., *Phys. Rev. B*, **35** (1987) 9683.
2. XANTHAKIS, J. P., PAPADOPOULOS, S. & MASON, P. R., *J. Phys. C: Solid State Phys.*, **21** (1988) L555.
3. MAKLER, S. S., MARTINS DA ROCHA, G. & ANDA, E. V., *Phys. Rev. B*, (**41**) 1990, 5857.
4. SOKEL, R. J., *J. Phys. Chem. Solids*, **41** (1980) 899.
5. ROBERTSON, J., *Philos. Mag.*, **44** (1981) 215.
6. REN, S. Y. & CHING, W. Y., *Phys. Rev. B*, **23** (1981) 5454.
7. XU, Y. & CHING, W. Y., *Mater. Res. Soc. Symp. Proc.*, **105** (1988) 181.
8. XU, Y. & CHING, W. Y., *Physica B*, **150** (1988) 32.
9. XU, Y. & CHING, W. Y., *Phys. Rev. B*, **51** (1995) 17379.
10. ROBERTSON, J., *Philos. Mag.*, **P 63** (1991) 47.
11. WEINBERG, Z. A. & POLLAK, R. A., *Appl. Phys. Lett.*, **27** (1975) 254.
12. KÄRCHER, R., LEY, L. & JOHNSON, R. L., *Phys. Rev. B.*, **30** (1984) 1986.
13. HOFFMANN, R., *Solids and Surfaces: A Chemist's View of Bonding in Extended Structures*. VCH, New York, 1988.
14. ALBRIGHT, T. A., BURDETT, J. K. & WHANGBO, M. H., *Orbital Interactions in Chemistry*. Wiley, New York, 1985.
15. BENCO, L., *Solid State Commun.*, **94** (1995) 861.
16. BENCO, L., *Surf. Sci.*, **327** (1995) 274.
17. HARDIE, D. & JACK, K. H., *Nature*, **180** (1957) 332.
18. ANDRE, J. M., *J. Chem. Phys.*, **50** (1969) 1536.
19. WHANGBO, M. H. & HOFFMANN, R., *J. Am. Chem. Soc.*, **100** (1978) 6093.
20. WHANGBO, M. H., EVAIN, M., HUNGBANKS, T., KERTESZ, M., S. WIJEYESEKERA, S. D., WILKER, C., ZHENG, C. & HOFFMANN, R., *Extended Hückel Molecular, Crystal and Properties Package*. QCPE Program No. 571, Indiana University, 1988.
21. HOFFMANN, R., *J. Chem. Phys.*, **39** (1963) 1397.
22. TRONG ANH, N., ELIAN, M. & HOFFMANN, R., *J. Am. Chem. Soc.*, **110** (1978) 110.
23. GRÜN, R., *Acta Cryst. B.*, **35** (1979) 800.
24. RAMIREZ, R. & BÖHM, M. C., *Int. J. Quantum. Chem.*, **34** (1988) 571.
25. WIJEYESEKERA, S. D. & HOFFMANN, R., *Organometallics*, **3** (1984) 949.
26. PROSPERPIO, D. M., HOFFMANN, R. & PREUSS, P., *J. Am. Chem. Soc.*, **116** (1994) 9634.
27. MURNAGHAN, F. D., *Proc. Natl. Acad. Sci. U.S.A.*, **30** (1944) 244.
28. BIRCH, F., *J. Geophys. Res.*, **57** (1952) 227.
29. MADELUNG, O. (ed.), *Semiconductors Group IV Elements and III-V Compounds*, Data in Science and Technology, Vol. 1. Springer, Berlin, 1991.
30. DISTEFANO, T. H. & EASTMAN, D. E., *Phys. Rev. Lett.*, **27** (1971) 1560.
31. IBACH, H. & ROWE, J. E., *Phys. Rev. B*, **10** (1974) 710.
32. WIECH, G., *Solid State Commun.*, **52** (1984) 807.
33. PARK, C. H., CHEONG, B. H., LEE, K. H. & CHANG, K. J., *Phys. Rev. B*, **49** (1994) 4485.
34. RUIZ, E., ALVAREZ, S. & ALEMANY, P., *Int. J. Quantum. Chem.*, **52** (1994) 365.
35. XU, Y. N. & CHING, W. Y., *Phys. Rev. B*, **44** (1991) 11048.
36. LI, Y. P. & CHING, W. Y., *Phys. Rev. B*, **31** (1995) 2172.
37. BENCO, L., *J. Solid State Chem.*, **110** (1994) 58.
38. BENCO, L., *J. Solid State Chem.*, **111** (1994) 440.
39. HÄGLUND, J., GUILLERMET, A. F., GRIMVALL, G. & KÖRLING, M., *Phys. Rev. B*, **48** (1993) 11685.
40. SCHNEIDER, S. J. (ed.), *Engineered Materials Handbook, Vol. 4, Ceramics and Glasses*. ASM International, 1991.